Modeling of the German National Standard for High Pressure Natural Gas Flow Metering in Modelica®

von der Heyde, Michael[1] Schmitz, Gerhard[2] Mickan, Bodo[3]

[1]Institut für Elektrische Energiesysteme und Automation, TUHH, Germany, heyde@tuhh.de
[2]Institut für Thermofluiddynamik, TUHH, Germany, schmitz@tuhh.de
[3]Physikalisch-Technische Bundesanstalt, Germany, bodo.mickan@ptb.de

Abstract

The German national metrological institute Physikalisch-Technische Bundesanstalt uses a High Pressure Piston Prover as the primary standard for high pressure natural gas flow meters. The High Pressure Piston Prover measures the gas flow rate using the time a piston needs to displace a defined enclosed volume of gas in a cylinder. Fluctuating piston velocity during measurement can be a significant source of uncertainty if not considered in an appropriate way (Mickan et al., 2010). A computational model written in Modelica® was developed to investigate measures for the reduction of this uncertainty. Validation of the model shows good compliance of the piston velocity in the model with measured data for certain volume flow rates. Reduction of the piston weight, variation of the start valve switching time and integration of a flow straightener were found to reduce the piston velocity fluctuations in the model significantly.

Keywords: Modeling of Multi-Domain Physical Systems, Modelica®, High Pressure Piston Prover, High Pressure Natural Gas Flow Metering

1 Introduction

The German national primary standard for high pressure natural gas flow metering is a High Pressure Piston Prover (HPPP). It is used to calibrate transfer standards for high pressure natural gas flow metering and is traceable to the standards of length and time. The HPPP is described in the references (Schmitz and Aschenbrenner, 1990; Physikalisch Technische Bundesanstalt, 1991; Physikalisch- Technische Bundesanstalt, 2009). It is operated and owned by the German national metrological institute Physikalisch-Technische Bundesanstalt (PTB) and currently installed on the calibration site for gas flow meters pigsar™ in Dorsten, Germany. The calibration facility pigsar™ is also further described in the references (Uhrig et al., 2006; Mickan et al., 2008). Figure 1 shows a picture of the HPPP.

Figure 1. Picture of the High Pressure Piston Prover (Physikalisch- Technische Bundesanstalt, 2009).

The uncertainty of high pressure natural gas flow meters and therefore also the uncertainty of the HPPP as their primary standard in Germany is of major importance for the trade with natural gas.

2 The Calibration Setup Including the HPPP

The HPPP is the central element of the setup used to calibrate transfer standards. The HPPP consists basically of a piston in a cylinder. Several indicators are mounted on the cylinder to signal the piston position. The pressure and temperature at the HPPP are measured downstream of the cylinder. For the calibration process several other components need to be included in the setup and considered, such as the transfer standards, valves and a nozzle bank.

The HPPP can be operated with inlet pressures up to 90 bar and flow rates up to 480 m^3/h (Physikalisch Technische Bundesanstalt, 1991).

The whole calibration setup including the HPPP is shown in Figure 2.

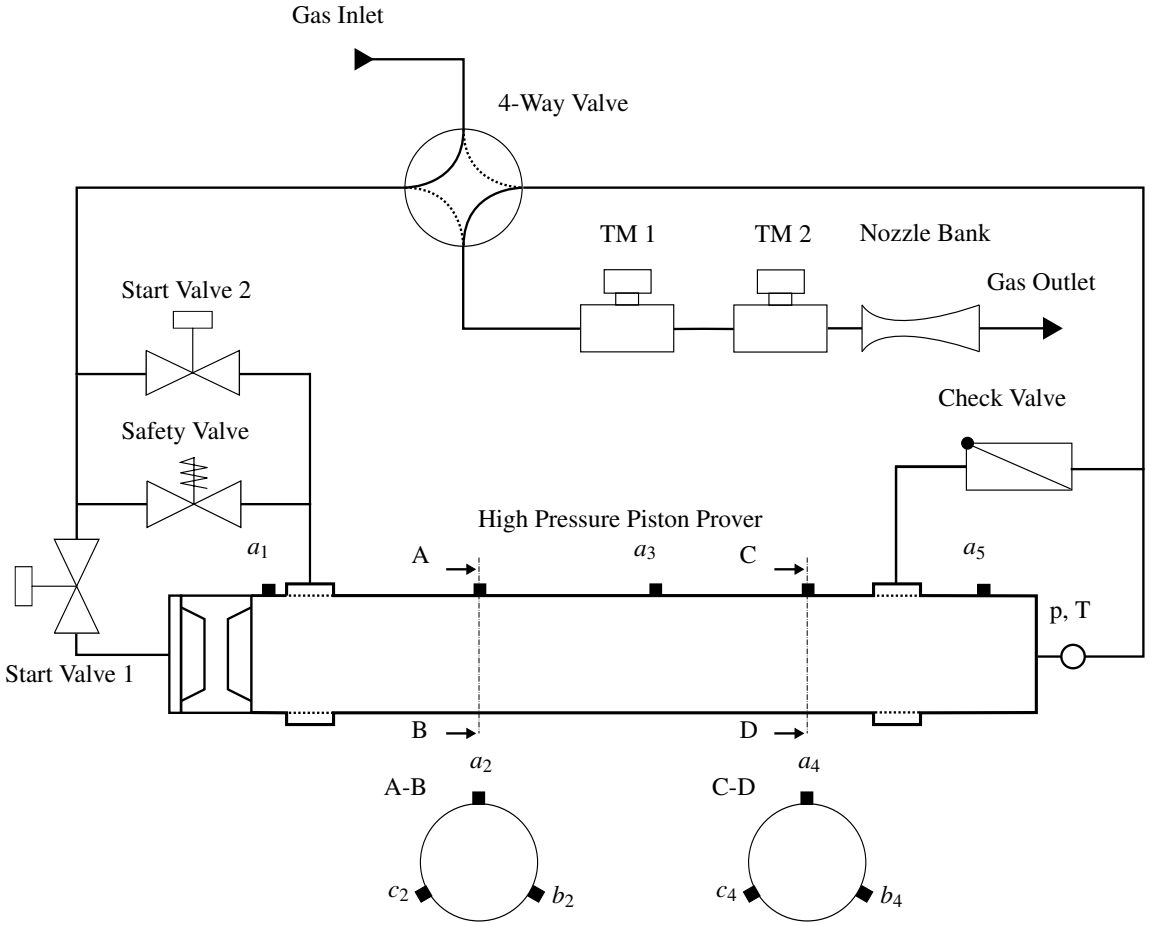

a_1, a_5	:	Position Indicator
a_2, b_2, c_2	:	Measurement Start Indicator
a_3	:	Half-Way Indicator
a_4, b_4, c_4	:	Measurement Stop Indicator

Figure 2. Scheme of the calibration setup using the High Pressure Piston Prover (Schmitz and Aschenbrenner, 1990).

Start valve 2 is used to initiate the movement of the piston, whereas start valve 1 is needed to prevent movement of the piston in between calibration runs due to the pressure drop across start valve 2. The 4-way valve is needed to revert the gas flow direction and move the piston back to its starting position after each calibration run. A check valve is used to prevent gas from flowing past the piston during the start of the reverse movement and a safety valve is included to prevent high forces on the piston at the end of the piston reverse movement.

Turbine Meters (TM) are used as transfer standards. TM measure the mass flow rate using the rotational speed of a turbine inserted in the fluid flow. The rotational speed of the turbine is metered using magnetically induced discrete signals. Two TM are connected in a row to minimize random measuring errors. The pressure at the TM is measured at their reference point and the temperature 2 diameters downstream of the TM.

The nozzle bank is used to set the flow rate. The critical nozzles are not necessary for the operation of the HPPP but provide the advantage to decouple the calibration setup from pressure fluctuations downstream of the nozzle bank. It consists of several critical flow nozzles in parallel connection. The pressure downstream of the nozzles is always low enough to ensure critical flow in the nozzles.

3 The Calibration Process

The closing of start valve 2 commences the running-in phase. The motion of the piston is indicated by the piston position indicator a_1. The measurement phase starts as the piston passes indicators a_2, b_2, c_2 and ends as the piston passes the indicators a_4, b_4, c_4. The volume flow rate is determined as stated in equation 1 from the vol-

DOI 10.3384/ecp15118663

ume in between the indicators V_{PP} and the time span $\Delta_{PP}t$ as given by the piston position indicator signals. It is therefore traceable to standards of length and time.

$$\dot{V}_{PP} = \frac{V_{PP}}{\Delta_{PP}t} \tag{1}$$

The signals of the TM are simultaneously counted. The volume flow rate $\dot{V}_{TM}$ can be determined using the relationship between the number of signals per time period indicated by the TM and the volume flow rate, known from previous calibration of the TM.

The calibration result is the relative deviation of the corrected volume flow rate as indicated by the TM $\dot{V}^c_{TM}$ and the corrected volume flow rate as indicated by the HPPP $\dot{V}^c_{PP}$. The relative deviation f is determined in equation 2. It can be used to correct the TM in further measurements or calibration steps.

$$f = \frac{\dot{V}^c_{TM} - \dot{V}^c_{PP}}{\dot{V}^c_{PP}} \tag{2}$$

Several corrections are used in equation 2 to improve the calibration accuracy. These corrections are explained in the following.

1. The volume flow rate indicated by the turbine meters $\dot{V}_{TM}$ is corrected as shown in equation 3 to prevent an error caused by the discrete nature of the TM signals. $\Delta_{PP}t$ is the duration of the measurement phase as determined from the piston position indicator signals. $\Delta_{TM}t$ is the time span from the first TM signal after the start of the measurement phase to the first TM signal after the end of the measurement phase.

$$\dot{V}^c_{TM} = \dot{V}_{TM}\frac{\Delta_{PP}t}{\Delta_{TM}t} \tag{3}$$

2. The temporal mean density over the measurement phase at the piston prover $\bar{\rho}_{PP}$ and at the TM $\bar{\rho}_{TM}$, both determined from measured pressure and temperature, are used to take the density changes along the gas flow direction into account as shown in the first term of equation 4.

$$\dot{V}^c_{PP} = \dot{V}_{PP}\frac{\bar{\rho}_{PP}}{\bar{\rho}_{TM}} + \frac{V_E}{\Delta_{PP}t}\frac{\rho_S - \rho_E}{\bar{\rho}_{TM}} \tag{4}$$

3. The temporal change of stored mass in between the cylinder and the TM during the measurement phase is taken into account as shown in the second term of equation 4, with V_E being the enclosed volume, ρ_S the spatial mean density in the enclosed volume at the start of the measurement phase and ρ_E the spatial mean density in the enclosed volume at the end of the measurement phase.

4 Uncertainty of the Calibration and Motivation for the Model

Several possible errors in the calibration process lead to the measurement uncertainty of the calibrated TM. These are

1. uncertainty in the determination of the volume in between piston position indicators,
2. uncertainty in the determination of the mean density,
3. repeatability of the TM measurement,
4. leakage between piston and cylinder,
5. dynamic error of the TM,
6. uncertainty in the determination of the stored mass in the enclosed volume.

The dynamic error of the TM is a consequence of the incorrect measurement of fast fluctuating volume flow rates due to turbine inertia. This error can be diminished using a mathematical correction method (Mickan et al., 2010), but the correction method as well leads to uncertainties.

The uncertainty of the calibrated transfer standards is 0.06 % (Physikalisch- Technische Bundesanstalt, 2009; Mickan et al., 2008). The last two listed errors combined lead to an uncertainty of 0.035% (Mickan et al., 2010). They are of dynamic nature and a consequence of piston velocity fluctuations. Figure 3 shows measured data for the piston velocity fluctuations in the measurement phase.

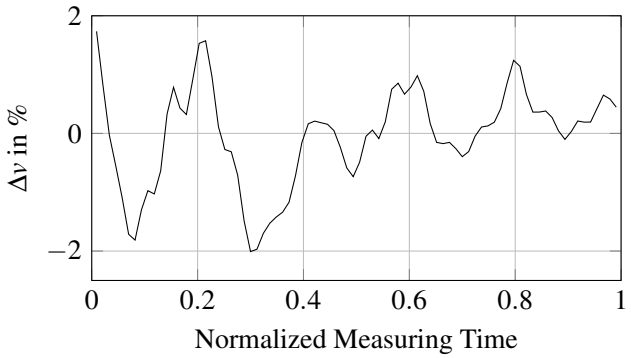

Figure 3. Relative deviation of the measured piston velocity from it's mean velocity Δv over the normalized measuring time.

The developed model is aimed to reproduce these piston velocity fluctuations and to find measures to reduce the fluctuations and therefore the uncertainty of the HPPP.

5 Description of the Model

Modelica® was chosen as the language to describe the dynamic and physical system. A graphical representation of the model is shown in Figure 4.

Several general assumptions were used in the model. Those are

1. pressure losses are proportional to the dynamic pressure,
2. the gas flow is one dimensional,
3. the system is adiabatic,
4. potential energy of the gas can be neglected,
5. no leakage occurs,
6. the heat transfer in the gas can be neglected in comparison to convective energy transport.

The gas at the inlet to the HPPP is assumed to have a constant temperature and pressure. This is consistent with data from measurements and is modeled using a supply volume of infinite size from the Modelica Standard Library (MSL). Equation 5 and 6 set these boundary conditions with T_{IN} being the inlet temperature and p_{IN} the inlet pressure.

$$T_{\mathrm{IN}} = \text{const.} \tag{5}$$

$$p_{\mathrm{IN}} = \text{const.} \tag{6}$$

The nozzle bank sets another boundary condition. It can be modeled as a single nozzle with a larger critical diameter. The used nozzles comply with ISO 9300 (International Organization for Standardization, 2005). The nozzle is modeled using a constant critical volume flow rate $\dot{V}_{\mathrm{N}}$ as shown in equation 7.

$$\dot{V}_{\mathrm{N}} = \text{const.} \tag{7}$$

Equation 8 is used to determine the mass flow through the nozzle $\dot{m}_{\mathrm{N}}$ from the critical volume flow rate $\dot{V}_{\mathrm{N}}$ and the upstream density ρ.

$$\dot{m}_{\mathrm{N}} = \dot{V}_{\mathrm{N}} \rho \tag{8}$$

The valves are taken from the MSL. They have a linear opening function $Y(t)$ and the mass flow $\dot{m}_{\mathrm{V}}$ is proportional to the pressure drop across the valve $\Delta_{\mathrm{V}} p$ as shown in equation 9 with $\dot{m}^n_{\mathrm{V}}$ and $\Delta^n_{\mathrm{V}} p$ being the nominal mass flow and pressure drop.

$$\dot{m}_{\mathrm{V}} = \Delta_{\mathrm{V}} p \frac{\dot{m}^n_{\mathrm{V}}}{\Delta^n_{\mathrm{V}} p} Y(t) \tag{9}$$

The start valves are used in the HPPP model to eliminate the influence of guessed initial conditions on the piston movement, as the stationary flow condition at the beginning of the running-in phase is not known.

The medium in the HPPP is natural gas. Due to the high pressure and high precision of the HPPP a real gas model is necessary. A Modelica Implementation of GERG 2008 with a constant gas composition out of 10 elements is used. GERG 2008 derives the equation of state for natural gas from the free energy. It is described in detail in the references (Kunz et al., 2007; Kunz and Wagner, 2012).

The enclosed gas volumes in the measuring cylinder change with piston movement. They can store mass m and internal energy mu as stated in equation 10 and 11. The volumes have i inlets or outlets. h is the specific enthalpy, v the mean velocity in a cross area A, p the static pressure and V the Volume. The pressure losses at inlets and outlets Δp are considered using constant coefficients ζ_{A} as shown in equation 12 with $\bar{\rho}$ being the mean density. No gradient for the thermodynamic state and no fluid friction is considered in the volumes.

$$\frac{\mathrm{d}m}{\mathrm{d}t} = \sum_{\mathrm{i}=1}^{\mathrm{n}} \dot{m}_{\mathrm{i}} \tag{10}$$

$$\frac{\mathrm{d}}{\mathrm{d}t}(mu) = \sum_{\mathrm{i}=1}^{\mathrm{n}} \dot{m}_{\mathrm{i}} \left(h_{\mathrm{i}} + \frac{v_{\mathrm{i}}^2}{2} \right) + p\dot{V} \tag{11}$$

$$\Delta p = \zeta_{\mathrm{A}} \frac{\bar{\rho}}{2} v_{\mathrm{A}}^2 \tag{12}$$

The position of the piston is determined from the equation of motion 13 with $F_{F,\mathrm{P}}$ being the friction force on the piston, $\Delta_{\mathrm{P}} p$ the pressures difference across the piston, A_{P} the piston cross area, m_{P} the piston weight and a_{P} the piston acceleration.

$$a_{\mathrm{P}} = \begin{cases} 0 & \text{for} \quad |F_{F,\mathrm{P}}| \geq |\Delta_{\mathrm{PP}} p| A_{\mathrm{P}} \\ \frac{\Delta_{\mathrm{P}} p A_{\mathrm{P}} - F_{F,\mathrm{P}}}{m_{\mathrm{P}}} & \text{for} \quad |F_{F,\mathrm{P}}| < |\Delta_{\mathrm{PP}} p| A_{\mathrm{P}} \end{cases} \tag{13}$$

The friction force on the piston is described as the sum of velocity independent coulomb friction F_C, velocity proportional friction $F_P v_{\mathrm{P}}$ and stribeck friction $F_S e^{-k v_{\mathrm{P}}}$ as stated in equation 14.

$$F_F = F_C + F_P v_{\mathrm{P}} + F_S e^{-k v_{\mathrm{P}}} \tag{14}$$

The coulomb friction F_C is modeled as a function of the piston position s_{P}. This function is determined by measuring the power consumption of a linear motor moving the piston slowly through the cylinder. Measured data is only available for 80 % of the cylinder length. After that the coulomb friction is assumed

DOI 10.3384/ecp15118663

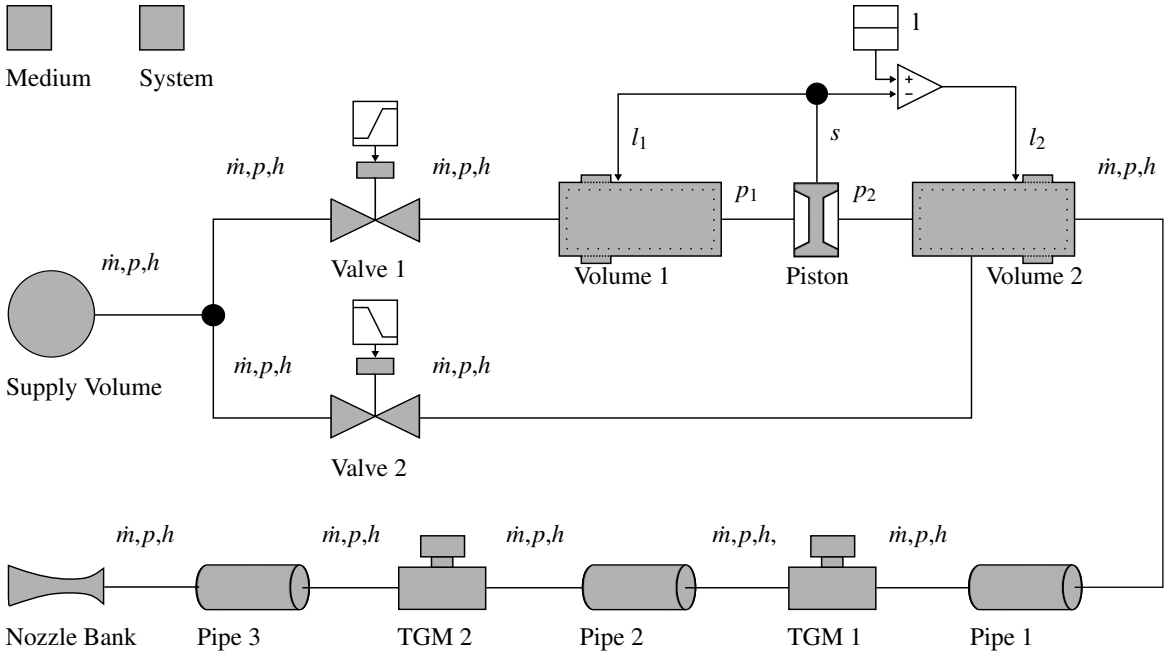

Figure 4. Graphical representation of the computational model.

constant. The measured coulomb friction is shown in Figure 5.

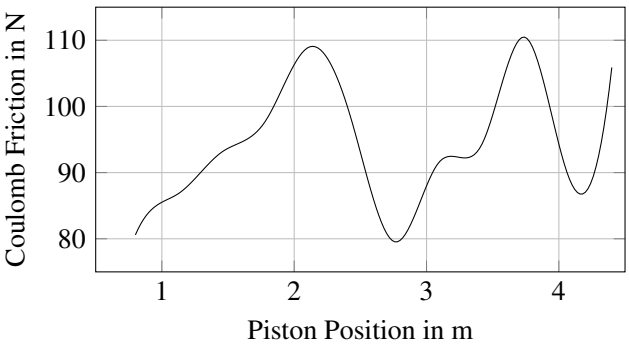

Figure 5. Measured coulomb friction as a function of the piston position.

The velocity proportional friction F_P was determined from measuring the pressure difference across the piston for different piston velocities and by linear interpolation of the measured data points.

The pipes are taken from the MSL. They can store mass m, internal energy mu and momentum mv as stated in equations 15, 16 and 17. A spatial discretisation in the direction of fluid flow is used, leading to a number of finite volumes in the pipe. Each volume reaches from cross area i to cross area $i+1$. In equation 15, 16 and 17 $\dot{m}$ is the mass flow, h the specific enthalpy, v the mean velocity, A the cross area, p the pressure and F_F the pipe friction force.

$$\frac{\mathrm{d}m}{\mathrm{dt}} = \dot{m}_\mathrm{i} + \dot{m}_{\mathrm{i}+1} \tag{15}$$

$$\frac{\mathrm{d}}{\mathrm{dt}}(mu) = \dot{m}_\mathrm{i} h_\mathrm{i} + \dot{m}_{\mathrm{i}+1} h_{\mathrm{i}+1} + \frac{1}{2}\left(vA\left(p_{\mathrm{i}+1} - p_\mathrm{i}\right) + vF_F\right) \tag{16}$$

$$\frac{\mathrm{d}}{\mathrm{dt}}(mv) = \dot{m}_\mathrm{i}|v_\mathrm{i}| + \dot{m}_{\mathrm{i}+1}|v_{\mathrm{i}+1}| - A\left(p_{\mathrm{i}+1} - p_\mathrm{i}\right) - F_F \tag{17}$$

The turbine meters are modeled using a constant pressure loss coefficient ζ_TM as stated in equation 18 with $\Delta_\mathrm{TM}p$ being the pressure loss, $\bar{\rho}$ the spatial mean density and v_A the mean velocity in the cross area A.

$$\Delta_\mathrm{TM}p = \zeta_\mathrm{TM}\frac{\bar{\rho}}{2}v_\mathrm{A}^2 \tag{18}$$

The pressure loss coefficient ζ_TM is taken from measurements. The relation between the indicated volume flow rate $\dot{V}_\mathrm{TM}^\mathrm{ind}$ and the true volume flow rate $\dot{V}_\mathrm{TM}$ in the TM can be modeled as shown in equation 19 (Mickan et al., 2010). The time constant τ is modeled as stated in equation 20 using a linear relation between the time constant and the initial mass flow $\dot{m}_\mathrm{IC}$ as approximately found in measurement.

$$\frac{d}{dt}\left(\dot{V}_\mathrm{TM}^\mathrm{ind}\right) = \frac{\dot{V}_\mathrm{TM}^\mathrm{ind} - \dot{V}_\mathrm{TM}}{\tau} \tag{19}$$

$$\tau = k\dot{m}_\mathrm{IC} \tag{20}$$

6 Verification of the Model

As measure for the verification and validation the relative deviation of the piston velocity from it's mean velocity in the measurement phase Δv is used. Δv represents the piston velocity fluctuations and is calculated as shown in equation 21 using the piston velocity v_P and the mean piston velocity $\bar{v}_\mathrm{P}$ determined from the distance Δl and the duration of the measurement phase Δt. For easy comparison of different volume flow rates a normalized time t_n is used in the figures. It is determined in equation 22 from the time t, the start time of the measurement phase t_s and the duration of the measurement phase Δt.

$$\Delta v = \frac{v_\mathrm{P} - \bar{v}_\mathrm{P}}{\bar{v}_\mathrm{P}} \quad \text{with} \quad \bar{v}_\mathrm{P} = \frac{\Delta l}{\Delta t} \tag{21}$$

$$t_\mathrm{n} = \frac{t - t_\mathrm{s}}{\Delta t} \tag{22}$$

For Integration the Solver Dassl included in Dymola® is used (Dassault Systemes, 2014) with a relative tolerance of 10^{-6}. Further decrease of the relative tolerance does not change the model trajectory as shown in Figure 6. No major change in the trajectories is detected when using other high order variable step solvers implemented in Dymola®.

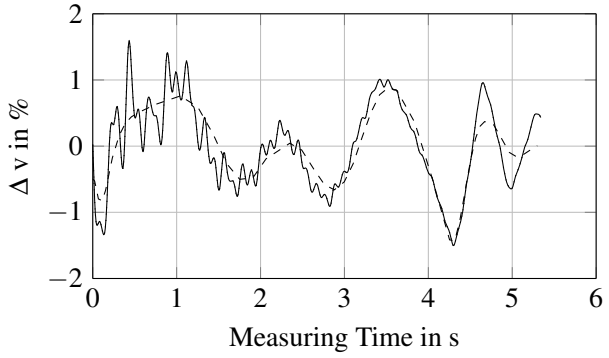

Figure 6. Relative deviation of the piston velocity from the mean velocity Δv in the model for different relative solver tolerances using Dassl.
- - - - $TOL = 10^{-4}$ —— $TOL = 10^{-6}$ —— $TOL = 10^{-8}$

Due to calculation time it is not functional to use a high number of finite pipe volumes in conjunction with real gas behavior. Here 4 discrete volumes in the first pipe and 2 volumes in the 2nd and 3rd pipe are used.

The verification of the model shows increasing frequency and decreasing deflection of the relative piston velocity deviation for increasing inlet pressures as shown in Figure 7.

Due to a shorter duration of the running-in phase, the piston velocity fluctuation resulting from piston acceleration remains active during the measuring phase for higher volume flow rates as shown in Figure 8.

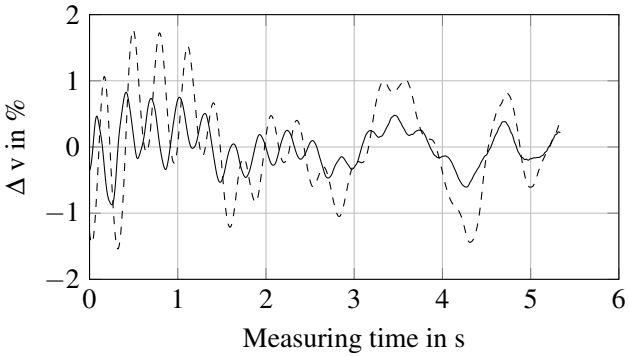

Figure 7. Relative deviation of the piston velocity from the mean velocity Δv in the model over the measuring time for different inlet pressures.
—— $p_\mathrm{IN} = 50\,\mathrm{bar}$ - - - - $p_\mathrm{IN} = 20\,\mathrm{bar}$

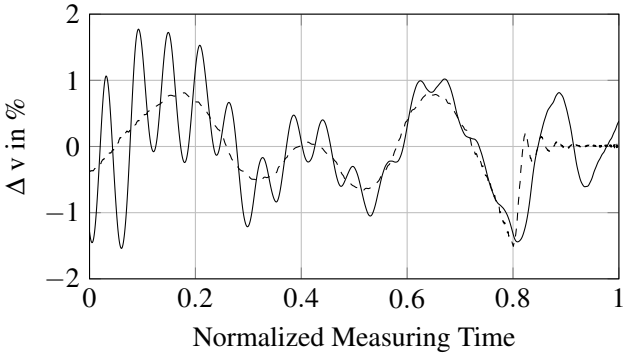

Figure 8. Relative deviation of the piston velocity from the mean velocity Δv in the model over the measuring time for different volume flow rates.
—— $\dot{V}_\mathrm{N} = 100\,\mathrm{m^3/h}$ - - - - $\dot{V}_\mathrm{N} = 25\,\mathrm{m^3/h}$

7 Validation of the Model

The model accuracy is highly relevant due to the low measuring uncertainty of the High Pressure Piston Prover. It depends on the uncertainty of the measured parameters used for the calibration of the model, the mentioned general assumptions, the simplified mathematical description and the accuracy of the numerical algorithm.

Measured data for the piston velocity is used to validate the model. The piston velocity was measured for volume flow rates up to $100\,\mathrm{m^3/h}$ using a laser distance measurement system.

The model validation shows relatively good accordance of the piston velocity fluctuations with measurement data for a volume flow rate of $100\,\mathrm{m^3/h}$, as

DOI 10.3384/ecp15118663

shown in Figure 9. The ground oscillation as well as the superimposed high frequency oscillation show similar characteristics for a volume flow rate of $100\,\mathrm{m}^3/\mathrm{h}$. This is also valid for different inlet pressures.

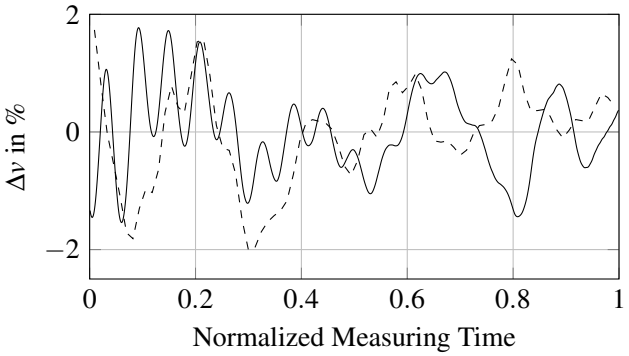

Figure 9. Comparison of the relative piston velocity deviation Δv over the normalized measuring time in the model and in measured data for a volume flow rate of $100\,\mathrm{m}^3/\mathrm{h}$ and an inlet pressure of 20 bar.
—— Simulation - - - - Measurement

For lower volume flow rates the model is not able to reproduce the measured piston velocity fluctuations. As an example the piston velocity fluctuation in the model is compared with measurement data for a volume flow rate of $25\,\mathrm{m}^3/\mathrm{h}$ in Figure 10. It can be seen, that the high frequency fluctuation in the measured data is not present in the model for a volume flow rate of $25\,\mathrm{m}^3/\mathrm{h}$.

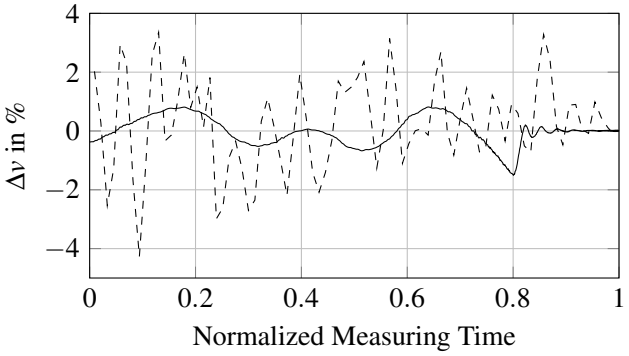

Figure 10. Comparison of the relative piston velocity deviation Δv over the normalized measuring time in the model and in measured data for a volume flow rate of $25\,\mathrm{m}^3/\mathrm{h}$ and an inlet pressure of 20 bar.
—— Simulation - - - - Measurement

Physical effects that are not included in the model and measurement uncertainties, both during the determination of the parameters for calibration and of the data for validation, might play an important role for low volume flow rates.

8 Constructional Means for Piston Velocity Fluctuation Reduction

The model is used to evaluate three different ways to reduce the piston velocity fluctuations in the measuring phase. The maximum deviation of the piston velocity from it's mean velocity $\Delta_{\max} v$ is used as a measure for the piston velocity fluctuations. The mean piston velocity deviation would not be an adequate measure here, as it does not limit the important piston velocity deviation at the start and end of the measurement phase, whereas the maximum piston velocity deviation does.

Accordingly to verification and validation the Solver Dassl included in Dymola® (Dassault Systemes, 2014) with a relative tolerance of 10^{-6} and 4 discrete volumes in the first pipe as well as 2 volumes in the 2nd and 3rd pipe are used.

Here the results for a volume flow rate of $100\,\mathrm{m}^3/\mathrm{h}$ and an inlet pressure of 20 bar are shown.

Figure 11 shows the maximum relative deviation of the piston velocity from it's mean velocity in the measuring phase for different piston weights. A lower piston weight leads to lower maximum piston velocity fluctuation in the model. The real piston weight is 21,7 kg. Reducing the piston weight by 50 % would lead to a significant drop of the piston velocity fluctuations. A way to achieve this reduction can be a change of the piston material from aluminum to fiber reinforced polymers.

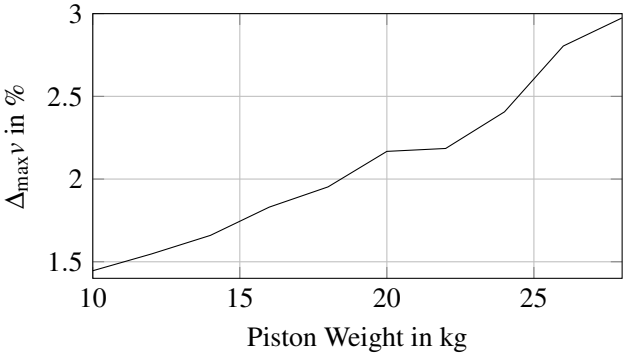

Figure 11. Maximum deviation of piston velocity from mean velocity in measuring phase for different piston weights.

Another way to reduce the piston velocity fluctuations in the model is shown in Figure 12. As can be seen, the switching time of start valve 1 has a strong influence on the maximum deviation of the piston velocity from its mean velocity during the measuring phase below a switching time of 0,4 s. The switching time would have to be be adopted for other volume flow rates using a controller.

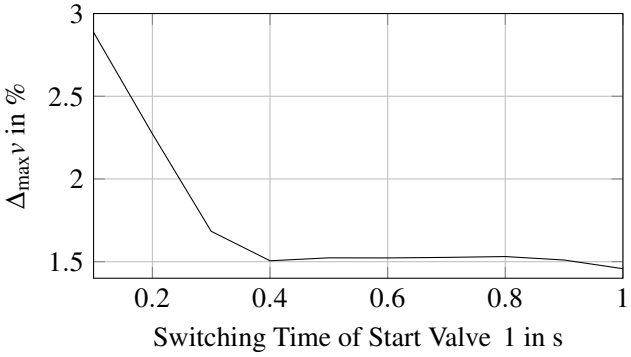

Figure 12. Maximum deviation of piston velocity from mean velocity in measuring phase for different switching times of start valve 1.

Figure 13 shows the maximum relative deviation of the piston velocity from it's mean velocity in the measuring phase as a function of the pressure loss coefficient of pipe 1. A significant reduction of the piston velocity fluctuations can be achieved for higher pressure loss coefficients. A possibility to raise the pressure loss coefficient would be the integration of a flow straightener. The error due to a higher pressure loss between the HPPP and the TM could be avoided using correction step 2 as described in section 3.

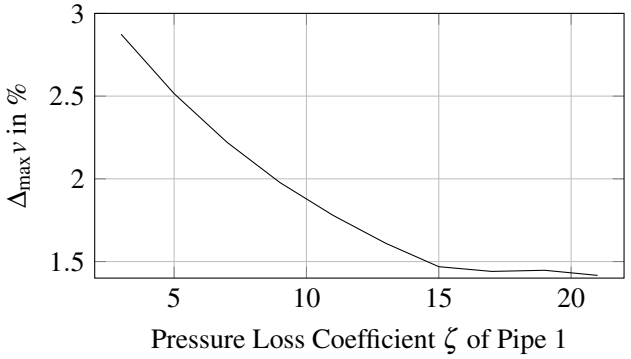

Figure 13. Maximum deviation of piston velocity from mean velocity in measuring phase for different pressure loss coefficients in pipe 1.

9 Conclusions

Modelica® proved the adequate language for the modeling of the High Pressure Piston Prover. It was possible to use several components from the Modelica Standard Library containing equations from various physical domains, such as tribology, thermodynamics and fluid flow. Parts of the model are replaceable and reusable due to Modelica® being object-oriented. The structure of the model follows the physical structure of the High Pressure Piston Prover closely. As a consequence of the Modelica® acausality the physical equations in the model are comprehensible and errors are easier located during the modeling process.

Three independent ways to reduce piston velocity fluctuations were demonstrated using the developed model. A significant reduction of the maximum piston velocity fluctuation during the measuring phase was found achievable by lowering the piston weight, an appropriate setting of the start valve switching time and the integration of a flow straightener. These measures are expected to reduce the High Pressure Piston Prover measuring uncertainty and can be realized with low effort.

References

Dassault Systemes. Dymola Dynamic Modeling Laboratory, 2014.

International Organization for Standardization. ISO 9300, 2005.

O. Kunz and W. Wagner. The GERG 2008 wide range equation of state for natural gases and other mixtures. *Journal of Chemical Engineering*, 2012.

O. Kunz, R. Klimeck, W. Wagner, and M. Jaeschke. The GERG 2004 wide range equation of state for natural gases and other mixtures. *GERG Technical Monograph*, 15, 2007.

B. Mickan, R. Kramer, H. Müller, V. Strunck, D. Vieth, and H.-M. Hinze. Highest precision for gas meter calibration worldwide: The high pressure gas calibration facility pigsar with optimized uncertainty. In *International Gas Union Research Conference*, 2008.

B. Mickan, R. Kramer, V. Strunck, and T. Dietz. Transient response of turbine flow meters during the application at a high pressure piston prover. In *15th Flow Measurement Conference (FLOMEKO)*, 2010.

Physikalisch- Technische Bundesanstalt. PTB mitteilungen, special issue volume 119 no.1, 2009.

Physikalisch Technische Bundesanstalt. Prüfschein der Rohrprüfstrecke, 1991.

G. Schmitz and A. Aschenbrenner. Experience with a piston prover as the new primary standard of the federal republic of germany in high pressure gas metering, 1990.

M. Uhrig, P. Schley, M. Jaeschke, D. Vieth, K. Altfeld, and I. Krajcin. High precision measurement and calibration technology as a basis for correct gas billing. In *23rd World Gas Conference*, 2006.